Inorganic Chemistry

Article

pubs.acs.org/IC

Metal Complexes (M = Zn, Sn, and Pb) of 2-Phosphinobenzenethiolates: Insights into Ligand Folding and Hemilability

Brian M. Barry,[†] Benjamin W. Stein,[†] Christopher A. Larsen,[†] Melissa N. Wirtz,[†] William E. Geiger,[‡] Rory Waterman,[‡] and Richard A. Kemp*[,†,§]

[†]Department of Chemistry and Chemical Biology, University of New Mexico, Albuquerque, New Mexico 87131, United States

[‡]Department of Chemistry, University of Vermont, Burlington, Vermont 05405, United States

[§]Advanced Materials Laboratory, Sandia National Laboratories, Albuquerque, New Mexico 87106, United States

Supporting Information

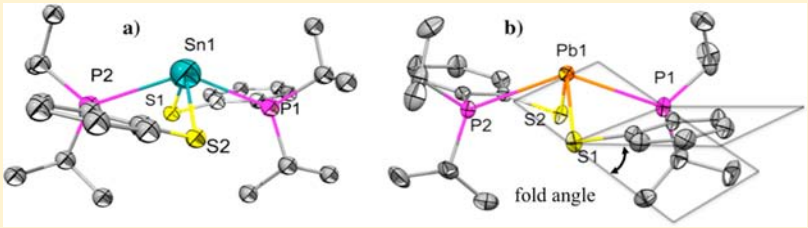

ABSTRACT: The divalent metal complexes $M^{II}\{(SC_6H_4\text{-}2\text{-}PR_2)\text{-}\kappa^2S,P\}_2$ (**3**–**7**, and **9**–**11**) (M = Zn, Sn, or Pb; R = ^{i}Pr, ^{t}Bu, or Ph), the Sn(IV) complexes $Sn\{(SC_6H_4\text{-}2\text{-}PR_2)\text{-}\kappa^2\text{-}S,P\}Ph_2Cl$ (**12** and **13**) (R = ^{i}Pr and ^{t}Bu), and the ionic Sn(IV) complexes $[Sn\{(SC_6H_4\text{-}2\text{-}PR_2)\text{-}\kappa^2\text{-}S,P\}Ph_2][BPh_4]$ (**14** and **15**) (R = ^{i}Pr and ^{t}Bu) have been prepared and characterized by multinuclear NMR spectroscopy and single crystal X-ray diffraction when suitable crystals were afforded. The Sn(II) and Pb(II) complexes with R = Ph, ^{i}Pr, or ^{t}Bu (**5**, **6**, **9**, and **10**) demonstrated ligand "folding" hinging on the P,S vector—a behavior driven by the repulsions of the metal/phosphorus and metal/sulfur lone pairs and increased M-S sigma bonding strength. This phenomenon was examined by density functional theory (DFT) calculations for the compounds in both folded and unfolded states. The Sn(IV) compound **13** (R = ^{t}Bu) crystallized with the phosphine in an axial position of the pseudotrigonal bipyramidal complex and also exhibited hemilability in the Sn–P dative bond, while compound **12** (R = ^{i}Pr), interestingly, crystallized with phosphine in an equatorial position and did not show hemilability. Finally, the crystal structure of **15** (R = ^{t}Bu) revealed the presence of an uncommon, 4-coordinate, stable Sn(IV) cation.

INTRODUCTION

Unsymmetric, multidentate ligands have garnered significant attention recently, in particular because of a subset of these ligands that exhibits hemilability.[1−4] In these hemilabile systems a hybrid ligand containing one strongly binding donor and one relatively weak donor can be employed to stabilize a metal center until a substrate is introduced.[5] Crucial to this process are the dynamic interactions between the metal center and the weak donor, whereby the chelate can open during reactions but remain closed, suppressing the active metal site, in the ground state structure.[5,6]

Transition-metal complexes employing hemilabile ligands have been well-studied, and have been successfully used, for example, as homogeneous catalysts for olefin metathesis,[7,8] for small molecule sensing,[9] and as catalysts for Suzuki–Miyaura coupling reactions.[10] The majority of the bifunctional ligands used in such transition-metal complexes are neutral with one hard and one soft donor, as in phosphine-amine or phosphine-ether ligand combinations.[5,6] N-heterocyclic carbene-substituted pincer complexes containing hemilabile pendant arms are also well documented.[11] Far less explored are main-group metal complexes having hemilabile ligands, with only a limited number of examples in the literature.[12−15]

We have previously reported that the Sn(II) complex $Sn[\{(^iPr_2P)_2N\}\text{-}\kappa^2\text{-}P,P]_2$ can form a CO_2 "adduct" by formal insertion of CO_2 into a Sn–P bond.[16] We have termed this complex a CO_2 adduct as the CO_2 molecule is quite labile in binding to and releasing from the metal fragment. This adduct formation is dependent upon the complex having an available Lewis base to form a dative interaction with the electrophilic central carbon atom of CO_2, while one nucleophilic oxygen atom of CO_2 can coordinate to the Lewis acidic metal center. This interesting reactivity has inspired us to explore alternative ligands that might behave similarly in their CO_2 reactivity. Of these possible ligands, the unsymmetric 2-phosphinobenzenethiolates (Scheme 1) that can chelate to main group metals via the neutral P and anionic S donor sites seemed particularly promising. These ligands would also have the potential to exhibit hemilability with the covalently bound thiolate acting as

Received: April 21, 2013
Published: August 12, 2013

   dx.doi.org/10.1021/ic400990n | *Inorg. Chem.* 2013, 52, 9875–9884

Scheme 1. Outline for Reactions Targeting M^{II} Complexes (3−7 and 9−11)

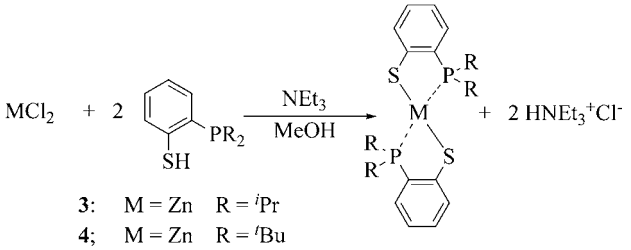

3: M = Zn R = ^{i}Pr
4; M = Zn R = ^{t}Bu
5: M = Sn R = ^{i}Pr
6: M = Sn R = ^{t}Bu
7: M = Sn R = Ph
9: M = Pb R = ^{i}Pr
10: M = Pb R = ^{t}Bu
11: M = Pb R = Ph

a strong donor and the phosphine acting as a weaker, more labile donor. The promise of these ligands was also substantiated by a recent report in which a related phenolate analogue was employed in an ionic zirconocene complex, demonstrating CO_2 insertion into the weak Zr−P bond to form a cyclic Zr phosphinocarbonate.[17]

While there have been many reports of complexes containing 2-phosphinobenzenethiolates in transition-metal complexes,[1,18−23] the use of this ligand type with main-group metals[24−30] is surprisingly rare. Using transition metals, all of the known examples are limited to the 2-(diphenylphosphino)-benzenethiolate ligand with one exception, that exception being a single report of a 2-phosphinobenzenethiolate complex in which the phosphine has isopropyl groups and is ligated to Rh and Ir.[31] In this report we expand the number of substituted 2-phosphinobenzenethiolate ligands and additionally report their reaction chemistry with several divalent metals (M = Zn(II), Sn(II) or Pb(II), **3**−**7** and **9**−**11**). As well, we prepared two higher-valent neutral Sn(IV) complexes (**12**−**13**), leading to cationic complexes after halide removal (**14**−**15**). Unfortunately and quite surprisingly to us, these complexes showed no tendency to react with CO_2. However, despite the lack of reactivity with CO_2 we did observe in the solid-state structure a unique example of ligand folding, as well as rare examples of hemilability between phosphine donors and Pb(II) and Sn(IV) metal centers, and formation of a stable coordinatively unsaturated Sn(IV) cation.

EXPERIMENTAL SECTION

General Procedures. Standard inert atmosphere and Schlenk techniques were used, as all reagents and products were presumed to be air and/or moisture-sensitive. The ligands 2-$Ph_2P(C_6H_4)SH$ and 2-$^t Bu_2P(C_6H_4)OH$ were prepared as previously reported.[32,33] Prior to use, cyclohexane and tetrahydrofuran (THF) (both Aldrich) were distilled from P_2O_5 and Na metal, respectively. Anhydrous methanol (EMD) was used as received while diethyl ether (Aldrich) was further dried using an LC Technology Solutions SP-105 purification system. All other reagents (Aldrich, Alfa-Aesar, or Strem) were used as-received without further purification. Solution ^1H, $^1H\{^{31}P\}$, $^{11}B\{^1H\}$, $^{13}C\{^1H\}$, $^{31}P\{^1H\}$, $^{119}Sn\{^1H\}$, and $^{207}Pb\{^1H\}$ NMR spectra were obtained on Bruker Avance 500 or Bruker Avance III 300 spectrometers. ^1H and $^{13}C\{^1H\}$ NMR were referenced to residual solvent peaks downfield of TMS. $^{11}B\{^1H\}$, $^{31}P\{^1H\}$, $^{119}Sn\{^1H\}$, and $^{207}Pb\{^1H\}$ spectra were referenced to external $BF_3{\cdot}Et_2O$, 85% H_3PO_4, $SnEt_4$, and $PbCl_{2(aq)}$, respectively. The solid state $^{31}P\{^1H\}$ spectrum was collected on an Avance III 300WB spectrometer. Melting points were measured under argon using a Uni-Melt capillary melting point apparatus. Infrared spectra were recorded on a Nicolet 6700 FT-IR spectrometer on KBr plates. Elemental analyses were obtained from Columbia Analytical Services located in Tucson, Arizona. For metal-containing compounds WO_3 was added to aid in oxidation during the CHN analyses; however, the C analyses for these Sn and Zn species were slightly lower than the calculated value, a phenomenon we have seen previously with a wide range of ligated main group complexes. Also consistent with our prior results is that the analyzed hydrogen levels appear not to be affected.

Synthesis of 2-$^i Pr_2P(C_6H_4)SH$ (1). This synthesis was performed with slight variation upon the previously reported synthesis of the analogous 2-$Ph_2P(C_6H_4)SH$.[32] 2-$^i Pr_2P(C_6H_4)SH$ has been previously prepared,[31] but without any synthetic details or characterization data provided. Thiophenol (8.00 g, 72.6 mmol) diluted to about 10 mL with cyclohexane was added dropwise to a stirred solution of 1.6 M *n*-butyllithium (100 mL, 160 mmol) and TMEDA (18.6 g, 160 mmol) in about 50 mL of cyclohexane at 0 °C. The solution stirred overnight, warming gradually to room temperature. The resulting white precipitate was isolated from the supernatant by filtration, washed with pentane and dried at atmospheric pressure for 1 h. It was then dissolved in 75 mL of THF and cooled to −78 °C whereupon a solution of $^i Pr_2PCl$ (7.75 g, 50.8 mmol) in about 10 mL of THF was added dropwise over 30 min. After stirring overnight and warming to room temperature, the resulting red-orange slurry was acidified by the addition of 0 °C, 1 M H_2SO_4. The aqueous layer of the resulting biphasic solution was washed twice with about 50 mL of diethyl ether and the combined organics (THF/diethyl ether) were then dried over $MgSO_4$ and concentrated in vacuo to afford a yellow oil. The product was distilled (ca. 20 mTorr) from the crude oil (80−100 °C) and collected as a yellow liquid. Yield 7.9 g (48%). ^1H (C_6D_6, 300 MHz): δ 0.84 (dd, $^3J_{P-H}$ = 15 Hz, $^3J_{H-H}$ = 6.9 Hz, 6H, $CH(CH_3)_2$), 1.05 (dd, $^3J_{P-H}$ = 15 Hz, $^3J_{H-H}$ = 6.9 Hz, 6H, $CH(CH_3)_2$), 1.88 (sept of d, $^2J_{P-H}$ = 2.4 Hz, $^3J_{H-H}$ = 6.9 Hz, 2H, $CH(CH_3)_2$), 5.10 (s, 1H, S*H*), 6.82−7.08 (m, 4H, C_6H_4). $^1H\{^{31}P\}$ (C_6D_6, 300 MHz): δ 0.84 (d, $^3J_{H-H}$ = 6.9 Hz, 6H, $CH(CH_3)_2$), 1.05 (d, $^3J_{H-H}$ = 6.9 Hz, 6H, $CH(CH_3)_2$), 1.88 (sept, $^3J_{H-H}$ = 6.9 Hz, 2H, $CH(CH_3)_2$), 5.10 (s, 1H, S*H*), 6.82−7.08 (m, 4H, C_6H_4). $^{13}C\{^1H\}$ ($CDCl_3$, 75 MHz): δ 19.1 (d, $^2J_{P-C}$ = 10 Hz, $CH(CH_3)_2$), 24.0 (d, $^2J_{P-C}$ = 10 Hz, $CH(CH_3)_2$), 25.8 (d, $^1J_{P-C}$ = 21 Hz, $CH(CH_3)_2$), 124.3 (s, C_6H_4), 128.8 (s, C_6H_4), 129.2 (s, C_6H_4), 133.0 (s, C_6H_4). $^{31}P\{^1H\}$ (C_6D_6, 121 MHz): δ −2.60 ppm. Anal. Calcd for $C_{12}H_{19}PS$: C, 63.68; H, 8.46. Found: C, 64.28; H, 8.37.

Synthesis of 2-$^t Bu_2P(C_6H_4)SH$ (2). Compound **2** was prepared in an analogous manner to **1**. The product was distilled (ca. 20 mTorr) from the crude oil (100−115 °C) and collected as a yellow liquid. Yield 8.9 g (48%). ^1H (C_6D_6, 300 MHz): 1.36 (d, $^3J_{P-H}$ = 12 Hz, 18H, $C(CH_3)_3$), 5.68 (s, 1H, S*H*), 6.78−7.11 (m, 4H, C_6H_4). $^{13}C\{^1H\}$ ($CDCl_3$, 75 MHz): 30.2 (d, $^2J_{P-C}$ = 13 Hz, $C(CH_3)_3$), 33.2 (d, $^1J_{P-C}$ = 17 Hz, $C(CH_3)_3$), 123.3 (s, C_6H_4), 129.0 (s, C_6H_4), 131.3 (s, C_6H_4),134.9 (s, C_6H_4). $^{31}P\{^1H\}$ (C_6D_6, 121 MHz) **2**: δ 18.8 ppm. Anal. Calcd for $C_{14}H_{23}PS$: C, 66.10; H, 9.41. Found: C, 66.28; H, 9.46.

Synthesis of $M^{II}\{(SC_6H_4\text{-}2\text{-}PR_2)\text{-}\kappa^2S,P\}_2$ (3−7, and 9−11). All divalent metal compounds were prepared in a similar manner in which the metal chloride, 10−15% molar excess of NEt_3, and the phosphinobenzenethiol were mixed in MeOH, resulting in the precipitation of pure product. A detailed synthesis of $Zn\{(SC_6H_4\text{-}2\text{-}P^iPr_2)\text{-}\kappa^2\text{-}S,P\}_2$ is given below, and the remaining divalent metal complexes are prepared in analogous fashion.

Synthesis of $Zn\{(SC_6H_4\text{-}2\text{-}P^iPr_2)\text{-}\kappa^2\text{-}S,P\}_2$ (3). Solid $ZnCl_2$ (0.139 g, 1.02 mmol) was added to a stirred solution of NEt_3 (0.237 g, 2.33 mmol) and **1** (0.460 g, 2.03 mmol) in about 25 mL of MeOH at room temperature. An immediate reaction occurs, resulting in a white precipitate. The reaction is allowed to stir for 15 h at room temperature. The white precipitate is then isolated by filtration, washed twice with diethyl ether (2 × 20 mL), and dried under vacuum for 1 h. Yield 0.420 g (80.1%). Colorless, single crystals of **3** were grown from a CH_2Cl_2/MeOH mixture. ^1H NMR (C_6D_6, 300 MHz): δ 0.87 (s, br, 12H, $CH(CH_3)_2$), 1.07 (s, br, 12H, $CH(CH_3)_2$), 1.98 (sept, br, 4H, $CH(CH_3)_2$), 6.38 (m, 2H, C_6H_4), 6.70 (m, 2H, C_6H_4), 6.83 (m, 2H, C_6H_4), 8.08 (m, 2H, C_6H_4). $^{13}C\{^1H\}$ (CH_2Cl_2, 75

dx.doi.org/10.1021/ic400990n | Inorg. Chem. 2013, 52, 9875−9884

MHz): δ 16.8 (s, $CH(CH_3)_2$), 18.1 (s, $CH(CH_3)_2$), 18.4 (s, $CH(CH_3)_2$), 19.1 (s, $CH(CH_3)_2$), 23.4 (d, $^1J_{P-C}$ = 55 Hz), 121.4 (s, C_6H_4), 130.4 (s, C_6H_4), 131.9 (s, C_6H_4), 132.9 (s, C_6H_4). $^{31}P\{^1H\}$ (C_6D_6, 121 MHz) δ 10.9 ppm. Anal. Calcd for $C_{24}H_{36}P_2S_2Zn$: C, 55.86; H, 7.03. Found: C, 55.66; H, 6.91. Mp 208−210 °C.

Synthesis of Zn{(SC_6H_4-2-P^{t}Bu$_2$)-κ^2-S,P}$_2$ (4). $ZnCl_2$ (0.080 g, 0.59 mmol), NEt_3 (0.137 g, 1.36 mmol) and **2** (0.300 g, 1.18 mmol) were reacted in MeOH as previously described, affording a white powder. Yield 0.205 g (60.8%). Colorless, single crystals of **4** were grown from a CH_2Cl_2/MeOH mixture. ^1H NMR ($CDCl_3$, 300 MHz): δ 1.45 (d, $^3J_{P-H}$ = 14 Hz, 36H, $C(CH_3)_3$), δ 6.90 (m, 2H, C_6H_4), δ 7.11 (m, 2H, C_6H_4), δ 7.53 (m, 2H, C_6H_4), δ 7.68 (m, 2H, C_6H_4). $^1H\{^{31}P\}$ ($CDCl_3$, 300 MHz): δ 1.45 (s, 36H, $C(CH_3)_3$), δ 6.90 (m, 2H, C_6H_4), δ 7.11 (m, 2H, C_6H_4), δ 7.53 (m, 2H, C_6H_4), δ 7.68 (m, 2H, C_6H_4). $^{13}C\{^1H\}$ (CH_2Cl_2, 75 MHz): δ 29.8 (s, $C(CH_3)_3$), 35.0 (br, $C(CH_3)_3$), 120.6 (s, C_6H_4), 130.1 (s, C_6H_4), 133.2 (s, C_6H_4), 133.8 (s, C_6H_4). $^{31}P\{^1H\}$ ($CDCl_3$, 121 MHz) δ 31.7 ppm. Anal. Calcd for $C_{28}H_{44}P_2S_2Zn$: C, 58.78; H, 7.75. Found: C, 58.98; H, 7.77. Mp >220 °C.

Synthesis of Sn{(SC_6H_4-2-P^{i}Pr$_2$)-κ^2-S,P}$_2$ (5). $SnCl_2$ (0.198 g, 1.04 mmol), NEt_3 (0.243 g, 2.40 mmol), and **1** (0.473 g, 2.09 mmol) were reacted in MeOH as previously described, affording a very faintly yellow powder. Yield 0.450 g (75.7%). Colorless, single crystals of **5** were grown from a CH_2Cl_2/MeOH mixture. ^1H NMR (C_6D_6, 300 MHz): δ 0.94 (dd, $^3J_{P-H}$ = 16 Hz, $^3J_{H-H}$ = 6.9 Hz, 12H, $CH(CH_3)_2$), 1.28 (dd, $^3J_{P-H}$ = 16 Hz, $^3J_{H-H}$ = 6.9 Hz, 12H, $CH(CH_3)_2$), 2.16 (m, br, 4H, $CH(CH_3)_2$), 6.77 (m, 2H, C_6H_4), 6.95 (m, 4H, C_6H_4), 7.88 (m, 2H, C_6H_4). $^1H\{^{31}P\}$ (C_6D_6, 300 MHz): δ 0.94 (d, $^3J_{H-H}$ = 6.9 Hz, 12 H $CH(CH_3)_2$), 1.28 (d, $^3J_{H-H}$ = 6.9 Hz, 12 H $CH(CH_3)_2$), 2.16 (m, br, 4H, $CH(CH_3)_2$), 6.77 (m, 2H, C_6H_4), 6.95 (m, 4H, C_6H_4), 7.88 (m, 2H, C_6H_4). $^{13}C\{^1H\}$ (CH_2Cl_2, 75 MHz): δ 18.6 (d, $^1J_{P-C}$ = 20 Hz, $CH(CH_3)_2$), 23.9 (s, $CH(CH_3)_2$), 122.8 (s, C_6H_4), 129.9 (s, C_6H_4), 132.9 (s, C_6H_4), 133.1 (s, C_6H_4). $^{31}P\{^1H\}$ (C_6D_6, 121 MHz) δ −2.87 ppm (s, Sn satellites, $^1J_{Sn-P}$ = 892 Hz). $^{119}Sn\{^1H\}$ (CH_2Cl_2, 112 MHz) δ −231.4 ppm (t, $^1J_{P-Sn}$ = 892 Hz). Anal. Calcd for $C_{24}H_{36}P_2S_2Sn$: C, 50.63; H, 6.37. Found: C, 50.86; H, 6.25. Mp 190−192 °C.

Synthesis of Sn{(SC_6H_4-2-P^{t}Bu$_2$)-κ^2-S,P}$_2$ (6). $SnCl_2$ (0.123 g, 0.65 mmol), NEt_3 (0.151 g, 1.49 mmol), and **2** (0.330 g, 1.30 mmol) were reacted in MeOH as previously described, affording a faintly yellow powder. Yield 0.358 g (88.2%). Colorless, single crystals of **6** were grown from a CH_2Cl_2/MeOH mixture. ^1H NMR ($CDCl_3$, 300 MHz) δ 1.41 (m, br, 36H, $C(CH_3)_3$), 6.95 (m, 2H, C_6H_4), 7.15 (m, 2H, C_6H_4), 7.52 (m, 2H, C_6H_4), 7.63 (m, 2H, C_6H_4). $^1H\{^{31}P\}$ ($CDCl_3$, 300 MHz): δ 1.41 (s, 36H, $C(CH_3)_3$), 6.95 (m, 2H, C_6H_4), 7.15 (m, 2H, C_6H_4), 7.52 (m, 2H, C_6H_4), 7.63 (m, 2H, C_6H_4). $^{13}C\{^1H\}$ (CH_2Cl_2, 75 MHz): δ 27.5 (s, $C(CH_3)_3$), 29.8 (br, $C(CH_3)_3$), 122.0 (s, C_6H_4), 129.5 (s, C_6H_4), 133.6 (s, C_6H_4), 135.7 (s, C_6H_4). $^{31}P\{^1H\}$ (CH_2Cl_2, 121 MHz) δ 16.8 ppm (s, Sn satellites, $^1J_{Sn-P}$ = 896 Hz). $^{119}Sn\{^1H\}$ (CH_2Cl_2, 112 MHz) δ −204.3 ppm (t, $^1J_{P-Sn}$ = 896 Hz). Anal. Calcd for $C_{28}H_{44}P_2S_2Sn$: C, 53.77; H, 7.09. Found: C, 53.97; H, 6.84. Mp >220 °C.

Synthesis of Sn{(SC_6H_4-2-PPh$_2$)-κ^2-S,P}$_2$ (7). $SnCl_2$ (0.188 g, 0.99 mmol), NEt_3 (0.228 g, 2.20 mmol), and 2-$Ph_2P(C_6H_4)SH$ (0.583 g, 1.98 mmol) were reacted in MeOH as previously described to afford an off-white powder. Yield 0.621 g (68.5%). Colorless, single crystals of **7** were grown from a CH_2Cl_2/MeOH mixture. ^1H NMR ($CDCl_3$, 300 MHz): δ 6.87 (d, $^3J_{H-H}$ = 7.4 Hz, 2H, PC_6H_4S), 6.97 (t, $^3J_{H-H}$ = 7.4 Hz, 2H, PC_6H_4S), 7.06 (t, $^3J_{H-H}$ = 7.4 Hz, 2H, PC_6H_4S), 7.18 (d, $^3J_{H-H}$ = 7.4 Hz, 2H, PC_6H_4S), 7.35−7.48 (m, 20H, C_6H_5). $^{13}C\{^1H\}$ ($CDCl_3$, 75 MHz): δ 124.2, 128.7, 129.6, 129.9, 131.3, 133.1, 133.5, 133.7, and 149.7 (singlets, aromatic *C*). $^{31}P\{^1H\}$ ($CDCl_3$, 121 MHz) δ −2.10 ppm (s, Sn satellites, $^1J_{Sn-P}$ = 640 Hz). $^{119}Sn\{^1H\}$ (C_6H_6, 112 MHz) δ −135.0 (t, $^1J_{P-Sn}$ = 640 Hz). Anal. Calcd for $C_{36}H_{36}P_2S_2Sn$: C, 61.30; H, 4.00. Found: C, 60.81; H, 3.94. Mp 163−165 °C.

Synthesis of Sn{(OC_6H_4-2-P^{t}Bu$_2$)-κ^2-O,P}$_2$ (8). Solid $SnCl_2$ (0.199 g, 1.05 mmol) was added to a stirred solution of NEt_3 (0.244 g, 2.41 mmol) and 2-^{t}Bu$_2$P(C_6H_4)OH (0.500 g, 2.10 mmol) in about 25 mL of MeOH at room temperature. An immediate reaction occurs, resulting in a white precipitate. The reaction is allowed to stir for 15 h at room temperature. The white precipitate is then isolated by filtration, washed twice with diethyl ether (2 × 20 mL), and dried under vacuum for 1 h. Yield 0.473 g (76.0%). Colorless, single crystals of **8** were grown from a CH_2Cl_2/MeOH mixture. ^1H NMR (C_6D_6, 300 MHz): δ 1.29 (overlapping doublets, $^3J_{P-H}$ = 6.6 Hz, 36H, $C(CH_3)_3$), 6.66 (m, 2H, C_6H_4), 7.11 (m, 2H, C_6H_4), 7.26 (m, 2H, C_6H_4), 7.44 (m, 2H, C_6H_4). $^{13}C\{^1H\}$ (C_6D_6, 75 MHz): δ 30.2 (s, $C(CH_3)_3$), 35.4 (s, $C(CH_3)_3$), 115.9 (s, C_4H_6), 121.5 (s, C_4H_6), 132.5 (s, C_4H_6), 134.7 (s, C_4H_6). $^{31}P\{^1H\}$ (C_6D_6, 121 MHz) δ 9.41 ppm (s, Sn satellites, $^1J_{Sn-P}$ = 1256 Hz). $^{119}Sn\{^1H\}$ (C_6D_6, 112 MHz) δ −301.0 ppm (t, $^1J_{P-Sn}$ = 1256 Hz). Anal. Calcd for $C_{28}H_{44}P_2O_2Sn$: C, 56.68; H, 7.48. Found: C, 53.97; H, 6.84. Mp 142−145 °C.

Synthesis of Pb{(SC_6H_4-2-P^{i}Pr$_2$)-κ^2-S,P}$_2$ (9). $PbCl_2$ (0.123 g, 0.44 mmol), NEt_3 (0.103 g, 1.02 mmol), and **1** (0.200 g, 0.88 mmol) were reacted in MeOH as previously described, affording a light-yellow powder. Yield 0.172 g (59.0%). Yellow, single crystals of **9** were grown from a CH_2Cl_2/MeOH mixture. ^1H NMR (C_6D_6, 300 MHz): δ 0.95 (s, br, 12H, $CH(CH_3)_2$), 1.23 (s, br, 12H, $CH(CH_3)_2$), 2.26 (sept, $^3J_{H-H}$ = 6.6 Hz, 4H, $CH(CH_3)_2$), 6.71 (t, $^3J_{H-H}$ = 7.5 Hz, 2H, C_6H_4), 6.91 (d, $^3J_{H-H}$ = 7.5 Hz, 2H, C_6H_4), 6.98 (t, $^3J_{H-H}$ = 7.5 Hz, 2H, C_6H_4), 7.85 (d, $^3J_{H-H}$ = 7.5 Hz, 2H, C_6H_4). $^{13}C\{^1H\}$ (CH_2Cl_2, 75 MHz): δ 19.1 (s, br, $CH(CH_3)_2$), 24.8 (s, br, $CH(CH_3)_2$), 122.8 (s, C_6H_4), 129.8 (s, C_6H_4), 133.6 (s, C_6H_4), 135.1 (s, C_6H_4). $^{31}P\{^1H\}$ (C_7H_8, 121 MHz) δ 19.4 ppm, (C_7H_8, −80 °C, 121 MHz) δ 14.9 ppm (Pb satellites, $^1J_{Pb-P}$ = 711 Hz). Anal. Calcd for $C_{24}H_{36}P_2S_2Pb$: C, 43.82; H, 5.52. Found: C, 44.40; H, 5.06. Mp 212−215 °C.

Synthesis of Pb{(SC_6H_4-2-P^{t}Bu$_2$)-κ^2-S,P}$_2$ (10). $PbCl_2$ (0.227 g, 0.82 mmol), NEt_3 (0.190 g, 1.88 mmol), and **2** (0.415 g, 1.63 mmol) were reacted in MeOH as previously described, affording a light-yellow powder. Pale yellow single crystals were grown by slow diffusion of pentane into toluene. Yield 0.323 g (55.4%). ^1H NMR ($CDCl_3$, 300 MHz): δ 1.41 (s, br, 36H, $C(CH_3)_3$), 6.84 (t, $^3J_{H-H}$ = 7.5 Hz, 2H, C_6H_4), 7.14 (t, $^3J_{H-H}$ = 7.5 Hz, 2H, C_6H_4), 7.48 (d, $^3J_{H-H}$ = 7.5 Hz, 2H, C_6H_4), 7.59 (d, $^3J_{H-H}$ = 7.5 Hz, 2H, C_6H_4). $^{13}C\{^1H\}$ (CH_2Cl_2, 75 MHz): δ 30.3 (s, $C(CH_3)_3$), 36.9 (s, br, $C(CH_3)_3$), 121.8 (s, C_6H_4), 129.8 (s, C_6H_4), 136.2 (s, C_6H_4), 136.8 (s, C_6H_4). $^{31}P\{^1H\}$ (C_7H_8, 121 MHz) δ 59.4 ppm, (C_7H_8, −80 °C, 121 MHz) δ 31.1 ppm (Pb satellites, $^1J_{Pb-P}$ = 871 Hz). Anal. Calcd for $C_{28}H_{44}P_2S_2Pb$: C, 47.11; H, 6.21. Found: C, 47.70; H, 5.73. Mp >220 °C.

Synthesis of Pb{(SC_6H_4-2-PPh$_2$)-κ^2-S,P}$_2$ (11). $PbCl_2$ (0.286 g, 1.00 mmol), NEt_3 (0.226 g, 2.20 mmol), and 2-$Ph_2P(C_6H_4)SH$ (0.586 g, 1.99 mmol) were reacted in MeOH as previously described, affording a yellow powder. Yield 0.414 g (41.2%). ^1H NMR ($CDCl_3$, 300 MHz): δ 6.70−7.70 (m, 28 H, C_6H_4 and C_6H_5). $^{13}C\{^1H\}$ ($CDCl_3$, 75 MHz): δ 124.6, 128.6, 128.7, 129.3, 129.6, 133.4, 133.7, 133.9 (singlets, aromatic *C*). $^{31}P\{^1H\}$ (C_7H_8, 121 MHz) δ 9.73 ppm. Anal. Calcd for $C_{36}H_{36}P_2S_2Pb$: C, 54.46; H, 3.55. Found: C, 55.12; H, 4.00. Mp > 220 °C.

Synthesis of Sn{(SC_6H_4-2-P^{i}Pr$_2$)-κ^2-S,P}Ph$_2$Cl (12). A solution of Ph_2SnCl_2 (0.810 g, 2.36 mmol) in about 75 mL of MeOH was cooled to −78 °C upon which a solution of **1** (0.533 g, 2.36 mmol) and NEt_3 (0.274 g, 2.71 mmol) in 30 mL of MeOH was added dropwise over 30 min. Upon complete addition the reaction mixture was allowed to warm to room temperature, where it stirred for 15 h. The resulting white precipitate was isolated from the supernatant by filtration and washed with Et_2O (2 × 30 mL) and then dried at atmospheric pressure for 2 h. Yield 0.752 g (59.8%). Colorless, single crystals of **12** were grown from a CH_2Cl_2/MeOH mixture. ^1H NMR (C_6D_6, 300 MHz): δ 0.81 (dd, $^3J_{P-H}$ = 16.8 Hz, $^3J_{H-H}$ = 7.2 Hz, 6H, $CH(CH_3)_2$), 1.11 (dd, $^3J_{P-H}$ = 16.8 Hz, $^3J_{H-H}$ = 7.2 Hz, 6H, $CH(CH_3)_2$), 2.49 (sept of d, $^2J_{P-H}$ = 2.7 Hz, $^3J_{H-H}$ = 7.2 Hz, 2H, $CH(CH_3)_2$), 6.6−6.8 (m, 2H, PC_6H_4S), 6.93 (m, 1H, PC_6H_4S) 7.05−7.30 (m, 6H, $C_{Ph}H_{m,p}$), 7.86 (m, 1H, PC_6H_4S), 8.58 (d, Sn satellites, $^3J_{H-H}$ = 1.2 Hz, $^3J_{Sn-H}$ = 92 Hz, 4H, $C_{Ph}H_o$). $^{13}C\{^1H\}$ (CH_2Cl_2, 75 MHz): δ 17.4 (s, $C(CH_3)_2$), 17.9 (s, $C(CH_3)_2$), 24.7 (d, $^1J_{P-C}$ = 18 Hz, $C(CH_3)_2$), 123.7, 128.6, 129.6, 131.9, 133.0, 136.0, 142.9 (singlets, all aromatic *C*). $^{31}P\{^1H\}$ (C_6D_6, 121 Hz) δ 10.8 ppm (s, $^1J_{Sn-P}$ = 637 Hz). $^{119}Sn\{^1H\}$ (C_6D_6, 112 MHz) δ −239.3 ppm (d, $^1J_{P-Sn}$ = 637 Hz). Anal. Calcd for

dx.doi.org/10.1021/ic400990n | Inorg. Chem. 2013, 52, 9875−9884

Table 1. Crystallographic Data and Parameters for Divalent Metal Complexes 3−10

	3	4	5	6	7	8	9	10
empirical formula	$C_{24}H_{36}P_2S_2Zn$	$C_{28}H_{44}P_2S_2Zn$	$C_{24}H_{36}P_2S_2Sn$	$C_{28}H_{44}P_2S_2Sn$	$C_{36}H_{28}P_2S_2Sn$	$C_{28}H_{44}O_2P_2Sn$	$C_{24}H_{36}P_2PbS_2$	$C_{28}H_{44}P_2PbS_2$
FW	515.96	572.06	569.28	625.38	705.33	593.26	657.78	713.88
T, K	173(2)	173(2)	172(2) K	173(2)	173(2)	100(2)	173(2)	173(2)
cryst size (mm)	0.51 × 0.32 × 0.23	0.31 × 0.25 × 0.15	0.35 × 0.28 × 0.14	0.30 × 0.21 × 0.18	0.34 × 0.27 × 0.20	0.26 × 0.16 × 0.14	0.65 × 0.48 × 0.44	0.41 × 0.37 × 0.31
cryst syst	monoclinic	monoclinic	monoclinic	monoclinic	triclinic	monoclinic	monoclinic	monoclinic
space group	$P2(1)/n$	$C2/c$	$P2(1)/c$	$P2(1)/c$	$P\bar{1}$	$P2(1)/c$	$P2(1)/c$	$P2(1)/c$
a, Å	7.9370(2)	26.861(2)	11.6509(13)	15.6438(7)	9.7365(11)	17.6554(15)	11.6851(6)	12.6418(2)
b, Å	15.6717(4)	8.0179(7)	15.1676(17)	12.3176(6)	9.8591(11)	12.5442(10)	15.2737(9)	15.5866(3)
c, Å	21.0443(5)	15.7280(13)	15.5835(19)	16.1013(6)	19.280(2)	14.4723(11)	15.4587(9)	16.0995(3)
α, deg	90.00	90.00	90.00.	90.00	100.037(4)	90.00	90.00	90.00
β, deg	98.8210(10)	122.853(5)	96.802(6).	103.031(2)	90.502(4)	113.782(5)	96.519(3)	106.7510(10)
γ, deg	90.00	90.00	90.00.	90	118.155(4)	90.00	90.00	90
vol, Å^3	2586.66(11)	2845.6(4)	2734.5(5)	3022.7(2)	1597.9(3)	2933.1(4)	2741.1(3)	3037.68(9)
Z	4	4	4	4	2	4	4	4
calcd density (g/cm^3)	1.325	1.335	1.383	1.374	1.466	1.343	1.594	1.561
μ, mm^{-1}	1.244	1.138	1.213	1.104	1.055	1.002	6.433	5.811
R1 $[I > 2\sigma(I)]^a$	0.0312	0.0402	0.0237	0.0669	0.0318	0.0618	0.0219	0.0221
wR2 $[I > 2\sigma(I)]^b$	0.0749	0.1068	0.0647	0.1803	0.0904	0.1466	0.0527	0.0485

^{a}R1 = $\sum||F_o| - |F_c||/\sum|F_o|$. ^{b}wR2 = $\{\sum[w(F_o^2 - F_c^2)^2]/\sum[w(F_o^2)^2]\}^{1/2}$.

$C_{24}H_{28}ClPSSn$: C, 54.01; H, 5.29. Found: C, 53.07; H, 5.29. Mp 140−142 °C.

Synthesis of Sn{(SC$_6$H$_4$-2-P^{t}Bu$_2$)-κ^2-S,P}Ph$_2$Cl (13). Ph_2SnCl_2 (0.656 g, 1.91 mmol), **2** (0.485 g, 1.91 mmol), and NEt_3 (0.222 g, 2.19 mmol) were reacted in MeOH as previously described for the synthesis of **12**, affording a white powder. Yield 0.815 g (76.1%). Colorless, single crystals of **13** were grown from a CH_2Cl_2/MeOH mixture. ^{1}H NMR ($CDCl_3$, 300 MHz): δ 1.32 (d, $^3J_{P-H}$ = 14.7 Hz, 9H, $C(CH_3)_3$), 1.36 (d, $^3J_{P-H}$ = 14.7 Hz, 9H, $C(CH_3)_3$) doublets at 1.32 and 1.36 ppm overlap, 7.0−8.3 (m, 14 H, PC_6H_4S and C_6H_5). ^{13}C{^{1}H} (CH_2Cl_2, 75 MHz): δ 29.5 (s, br, $C(CH_3)_2$), 37.1 (s, br, $C(CH_3)_2$), 123.3, 128.9, 129.7, 131.1, 134.8, 135.7, 145.6 (singlets, all aromatic C). ^{31}P{^{1}H} (CH_2Cl_2, 121 Hz): δ 20.5 (s, Sn satellites, $^1J_{Sn-P}$ = 389 Hz), 71.2 (s, Sn satellites, $^4J_{Sn-P}$ = 67 Hz). ^{31}P{^{1}H} (solid state) δ 12.9 (s, Sn satellites, $^1J_{Sn-P}$ = 1030 Hz). ^{119}Sn{^{1}H} (CH_2Cl_2, 112 MHz): δ −260.6 (s, br), −264.4 (s, br). Anal. Calcd for $C_{26}H_{32}ClPSSn$: C, 55.59; H, 5.74. Found: C, 54.67; H, 5.47. Mp 186−189 °C.

Synthesis of [Sn{(SC$_6$H$_4$-2-P^{i}Pr$_2$)- κ^2-S,P}Ph$_2$][BPh$_4$] (14). Solid $NaBPh_4$ (0.277 g, 0.81 mmol) was added to a flask containing a solution of **12** (0.431 g, 0.81 mmol) dissolved in about 40 mL of CH_2Cl_2, resulting in a white slurry. This mixture was stirred for 15h at room temperature. The mixture was then filtered through Celite filter aid, and the resulting filtrate had the volatile components removed in vacuo, resulting in a white powder. Yield 0.556 g (84.1%). ^{1}H NMR (CD_2Cl_2, 300 MHz): δ 0.87 (m, br, 6H, $CH(CH_3)_2$), 1.14 (m, br, 6H, $CH(CH_3)_2$), 2.59 (m, br, 2H, $CH(CH_3)_2$), 6.85−7.85 (m, 34H, aromatic H). ^{11}B{^{1}H} (CH_2Cl_2, 96 MHz) δ −4.80. ^{31}P{^{1}H} (CH_2Cl_2, 121 Hz) δ 27.2 (s, Sn satellites, $^1J_{Sn-P}$ = 187 Hz). ^{119}Sn{^{1}H} (CH_2Cl_2, 112 MHz) δ −129.7 (d, $^1J_{P-Sn}$ = 187 Hz). Anal. Calcd for $C_{48}H_{48}BPSSn$: C, 70.53; H, 5.92. Found: C, 65.90; H, 5.80. Mp 138−140 °C.

Synthesis of [Sn{(SC$_6$H$_4$-2-P^{t}Bu$_2$)- κ^2-S,P}Ph$_2$][BPh$_4$] (15). $NaBPh_4$ (0.248 g, 0.72 mmol) and **13** (0.400 g, 0.72 mmol) were reacted in CH_2Cl_2 as previously described for **14**. Yield 0.516 g (85.1%). Colorless, single crystals of **15** were grown from a CH_2Cl_2/hexanes mixture. ^{1}H NMR (CD_2Cl_2, 300 MHz): δ 1.33 (d, $^3J_{P-H}$ = 17.4 Hz, 18H, $C(CH_3)_3$), 6.80−8.00 (m, 34H, aromatic H). ^{11}B{^{1}H} (CH_2Cl_2, 96 Hz) δ −6.91. ^{31}P{^{1}H} (CH_2Cl_2, 121 MHz) δ 53.9 (s, Sn satellites, $^1J_{Sn-P}$ = 130 Hz). ^{119}Sn{^{1}H} (CH_2Cl_2, 112 MHz) δ −66.50 (d, $^1J_{P-Sn}$ = 130 Hz). Anal. Calcd for $C_{50}H_{52}BPSSn$: C, 71.03; H, 6.20. Found: C, 69.73; H, 6.09. Mp 153−156 °C.

Atmospheric Pressure CO_2 Reactions. In separate reactions, CO_2 was bubbled through solutions of **3**−**7** and **9**−**15** (ca. 50−150 mg) dissolved in about 20 mL of CH_2Cl_2 for 1 h. The solutes from the resulting solutions were deposited on KBr plates by evaporation in an Ar atmosphere and then examined by FT-IR spectroscopy for the presence of new stretches in the C═O region not seen in samples prior to CO_2 bubbling.

Crystallographic Studies. The crystals (**3**−**10**, **12**, **13**, and **15**) were coated with Paratone-N oil and were mounted on the nylon fiber of a CryoLoop that had been previously attached to a metallic pin using epoxy. The data were collected at the temperatures indicated in the tables using a Bruker X8 Apex II diffractometer using monochromated Mo K_α radiation (λ = 0.71073 Å). Data collection and processing were done using the APEX2 software suite.[34] The structures were solved using direct methods and refined with the full-matrix least-squares method on F^2 with SHELXTL.[35] The non-hydrogen atoms were refined anisotropically. Hydrogen atoms were included at geometrically idealized positions and were not refined. The isotropic thermal parameters of the hydrogen atoms were fixed at 1.5U equiv. of parent atom for methyl group hydrogens and 1.2U equiv. for all others. All final crystallographic figures shown in this document were generated by Diamond, v. 3.2i.[36] Crystallographic data are given in Tables 1 and 2.

Computational Studies. Density functional theory (DFT) calculations were performed with ADF 2012.01.[37−39] The PBE GGA functional was used with an all-electron triple-ζ basis set (TZP).[40] Scalar relativistic effects were included self-consistently with the ZORA Hamiltonian .[41−43] Computational results were interpreted with the Natural Bond Order (NBO v5.0) package incorporated into ADF.[44,45]

RESULTS AND DISCUSSION

Preparation and Characterization of M(II) Complexes. The previously uncharacterized 2-^{i}Pr$_2$P(C_6H_4)SH (**1**) and unreported 2-^{t}Bu$_2$P(C_6H_4)SH (**2**) ligands were prepared in an analogous manner to procedures by Block et al.[32] and Figuly et al.[46] for the synthesis of 2-Ph$_2$P(C_6H_4)SH. Thiophenol can be *ortho*-dilithiated by ^{n}BuLi in the presence of TMEDA followed by the addition of the R_2PCl species, and the final product is obtained upon acidification. The literature procedure followed indicated a 10% excess of ^{n}BuLi in the first step was

dx.doi.org/10.1021/ic400990n | Inorg. Chem. 2013, 52, 9875−9884

Table 2. Crystallographic Data and Parameters for Sn(IV) complexes 12, 13, and 15

	12	13	15
empirical formula	$C_{24}H_{28}$ ClPSSn	$C_{26}H_{32}$ClPSSn	$C_{100}H_{104}B_2P_2S_2Sn_2$
FW	533.63	561.69	1690.89
T, K	173(2)	173(2)	173(2)
cryst size (mm)	0.57 × 0.31 × 0.18	0.24 × 0.15 × 0.12	0.51 × 0.34 × 0.09
cryst syst	triclinic	monoclinic	triclinic
space group	$P\bar{1}$	$P2(1)/n$	$P\bar{1}$
a, Å	9.0010(3)	9.0291(9)	11.4110(16)
b, Å	10.4139(4)	18.6489(19)	17.150(2)
c, Å	13.3513(5)	15.7053(14)	22.365(2)
α, deg	87.573(2)	90.00	78.620(7)
β, deg	74.666(2)	101.863(6)	89.925(7)
γ, deg	76.296(2)	90.00	82.993(8)
vol, Å^3	1172.31(7)	2588.0(4)	4257.5(9)
Z	2	4	2
calcd density (g/cm^3)	1.512	1.442	1.319
μ, mm^{-1}	1.369	1.244	0.720
R1 $[I > 2\sigma(I)]^a$	0.0326	0.0501	0.0549
wR2 $[I > 2\sigma(I)]^b$	0.0780	0.1276	0.1442

^{a}R1 = $\sum||F_o| - |F_c||/\sum|F_o|$. ^{b}wR2 = $\{\sum[w(F_o^2 - F_c^2)^2]/\sum[w(F_o^2)^2]\}^{1/2}$.

needed to produce 1-SLi-2-LiC_6H_4. Several years later it was found that the addition of another equivalent of ^{n}BuLi to 1-SLi-2-LiC_6H_4 produces a trilithiated cluster $[Li_3\{(2\text{-}S\text{-}C_6H_4)(CH_2MeNCH_2CH_2Me_2)(TMEDA)\}]_2$, containing a deprotonated TMEDA.[47] We suspected that even using the 10% excess might produce the trilithiated thiophenol as a side product, and this suspicion was confirmed when crystals of the trilithiated cluster were grown from the supernatant of our dilithiation route. While the presence of the trilithiated thiophenol did not prevent pure products from being obtained, it did lead to somewhat lowered yields. Isolation of analytically pure 2-^{i}Pr$_2$P(C_6H_4)SH (**1**) and 2-^{t}Bu$_2$(C_6H_4)SH (**2**) were achieved by vacuum distillation while 2-Ph$_2$P(C_6H_4)SH was purified by recrystallization.[32]

In the syntheses of the divalent metal complexes reported here, the addition of MCl_2 (M = Zn, Sn, and Pb) to a solution of 2-R$_2$P(C_6H_4)SH (R = ^{i}Pr, ^{t}Bu, and Ph) and excess NEt_3 in MeOH at room temperature resulted in an instantaneous reaction for both $ZnCl_2$ and $SnCl_2$, whereas the $PbCl_2$ reactions took a few minutes likely because of the relatively low solubility of $PbCl_2$ in MeOH (Scheme 1). Each product precipitates from methanol and can be isolated as an analytically pure product after washing. Some product is lost in the filtrate, as all products have some solubility in MeOH, but given the synthetic ease and resulting purity of the products, the loss is tolerable. For complexes **3**−**7** and **9**, suitable crystals for single crystal X-ray diffraction were grown from a CH_2Cl_2/MeOH mixed solvent system at −18 °C, while crystals for complex **10** were grown by slow vapor diffusion of pentane into a toluene solution. Although crystalline samples of **11** were obtained, none were of sufficient quality to allow structure determination.

Multinuclear NMR data were collected for species **3**−**7** and **9**−**11**; all showing singlets (−2.87 to 39.5 ppm) in the $^{31}P\{^1H\}$ spectra, thus indicating chemically equivalent phosphorus nuclei on adjacent ligands in the solution phase. For the Sn complexes **5**−**7**, corresponding $^1J_{Sn-P}$ coupling were observed in both the $^{119}Sn\{^1H\}$ and the $^{31}P\{^1H\}$ spectra with values of 892, 896, and 640 Hz, respectively, demonstrating P−Sn interaction in solution. The relative values of these coupling constants are congruent with what is expected based on the relative basicity of the P lone pair interacting with the acidic Sn center (-PR$_2$: ^{t}Bu > ^{i}Pr > Ph). The $^{119}Sn\{^1H\}$ shifts for **5**−**7** are −231.4, −204.3, and −135.0 respectively. The more downfield position of **7** can be rationalized by the relatively weaker basicity of the phosphine groups because of the presence of electron-withdrawing phenyl groups, leading to a more deshielded Sn center. When comparing **5** and **6**, basicity alone would anticipate a more upfield shift for **6**, but with **6** having slightly bulkier alkyl groups, sterics lead to slightly longer Sn−P bonds and a more deshielded Sn center.

Room temperature $^{31}P\{^1H\}$ NMR spectra of the Pb samples (**9**−**11**) all revealed singlets at 19.4, 59.4, and 9.73 ppm, respectively, surprisingly devoid of Pb satellites. Additionally, despite extensive run times, no ^{207}Pb NMR peaks could be detected for *any* of the Pb samples. The lack of distinct peaks could be indicative of a dynamic process between having the P in the bound and unbound states, which could broaden the ^{207}Pb signals to undetectable levels and is likely why Pb satellites were not observed. To probe this further, low-temperature (−80 °C) ^{31}P and ^{207}Pb NMR spectra were recorded for all three samples. Upon cooling, Pb satellites could easily be seen in the $^{31}P\{^1H\}$ NMR spectra for compounds **9** and **10** ($^1J_{Pb-P}$ 711 and 871 Hz, respectively); however, no satellites were observed in **11**, attributable to the relative decrease in basicity caused by the electron-withdrawing phenyl groups. The appearance of Pb satellites upon cooling in **9** and **10** is consistent with ligand hemilability, and is not surprising given the weak Lewis acidity of Pb(II). Again, even after extensive run times, no peaks were observed in the ^{207}Pb NMR spectra.

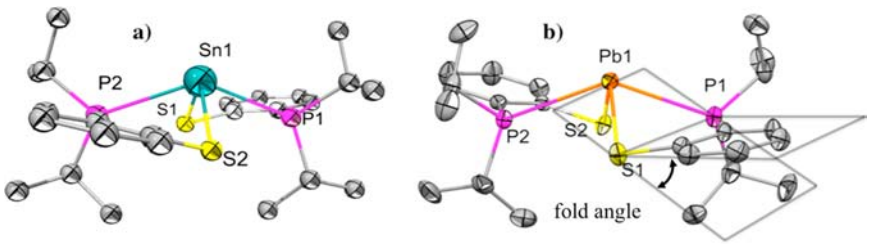

Figure 1. Molecular structures of **5** (a) and **9** (b) (50% ellipsoids). Hydrogen atoms omitted for clarity. Selected bond lengths (Å) and angles (deg). **5** (a): Sn(1)−P(1) 2.7936(5), Sn(1)−P(2) 2.8686(6), Sn(1)−S(1) 2.5481(6), Sn(1)−S(2) 2.5462(5), P(1)−Sn(1)−P(2) 139.340(16), S(1)−Sn(1)−S(1) 105.516(18). **9** (b): Pb(1)−P(1) 2.8705(5), Pb(1)−P(2) 2.9594(5), Pb(1)−S(1) 2.6344(6), Pb(1)−S(2) 2.6277(5), P(1)−Pb(1)−P(2) 137.797(15), S(1)−Pb(1)−S(2) 103.103(17). Visualization of the planes used to calculate the fold angle can be seen in (b).

dx.doi.org/10.1021/ic400990n | Inorg. Chem. 2013, 52, 9875−9884

Phosphorus-decoupled proton NMR experiments were performed on samples **4**, **5**, and **6** to help assign coupling constants for the alkyl signals in the nondecoupled spectra. In both samples **4** and **6**, a singlet resulted in the decoupled spectra indicating that all *t*-butyl groups are chemically equivalent and that splitting is in fact due to $^{3}J_{P-H}$ coupling. In the coupled spectrum of **5**, the diastereotopic methyl hydrogens on the isopropyl groups led to two doublets of doublets, with coupling of the methyl groups to both the methine hydrogen and the phosphorus. The decoupled spectra simplified to two doublets, both with coupling constants of 6.9 Hz ($^{3}J_{H-H}$), revealing that the constant of 16 Hz in the nondecoupled spectrum was due to $^{3}J_{P-H}$ coupling.

From the crystal structures (Figures 1, 3, Supporting Information, Figures S2 and S3), the geometry of the metal centers in the Sn(II) and Pb(II) complexes (**5**−**7**, **9**, and **10**) can all be similarly described as highly distorted trigonal bipyramidal with the axial positions being occupied by the P atoms and the equatorial positions by the two S atoms and one by the Sn or Pb lone pair. None of the bond lengths or angles in the structures of **5**−**7**, **9**, and **10** are particularly unexpected or out of the ordinary. Structurally characterized divalent metal benzenethiolates, particularly with transition metals, are extremely common, and hundreds of main group metal benzenethiolates have also been subjected to single crystal X-ray analysis. The most similar structurally characterized complexes to **5**−**7**, **9**, and **10**, in which the benzenethiolate contains an *ortho*-PR_2 moiety, are the related species reported by Zubieta et al.[25,26] or Morales-Morales et al.[30] For our complexes **5**−**7**, the Sn−S bond lengths fall in the range of 2.47−2.57 Å, quite similar to previous values of 2.473(3),[30] 2.494(1), and 2.503(1) Å reported earlier.[26] As well, our Pb−S bond lengths for **9** and **10** are in the range of 2.60−2.63 Å, essentially identical to earlier values of 2.6439(8) and 2.6462(7) Å from Zubieta et al..[25]

Upon further scrutiny of the crystal structures of these compounds, it was noticed that significant fold angles, reminiscent of those found in transition-metal dithiolenes,[48−50] were formed in the chelate rings. In these structures, the fold angle can be described as the acute angle formed between the M−S−P plane and the least-squares plane formed by S−C═C−P, with folding along the S−P vector (Figure 1). There are stark differences, however, between the system reported here and the aforementioned dithiolenes. The most obvious difference is that the dithiolenes are dianionic with two sulfurs as opposed to monoanionic with one sulfur and one phosphorus, as in our system. The other main difference is the nature of the metal centers: reports of dithiolenes with significant fold angles (<30°) are limited to early transition metals (M = Ti, Zr, Hf, V, Nb, Mo, and W),[48−62] and lanthanides/actinides (Ce, Nd, and U),[63,64] while our complexes are based on main-group metals.

Early transition-metal dithiolenes are reported to be stabilized by the bonding interaction of the lone pairs in filled S_{π} orbitals with an unoccupied M_d orbital that shares the M−S−S plane, the same interaction that gives rise to the folding.[48−50,59] The availability of a geometrically suited, unoccupied d orbital is the feature that limits the folding action to early transition metals (d^0 and d^1) and f element metals. Most transition-metal dithiolenes have fold angles less than 15° because of filled d-orbitals in the M−S−S plane.[50] Upon examination of the crystal structures of compounds **5** and **9** (Figure 1), **6** (Figure 3), and **10** (Supporting Information, Figure S3) we observed large fold angles (35−52°), but since we are dealing with s and p block main-group metals there must be an alternate explanation for the folding. Full DFT calculations were performed on compounds **5**, **6**, **9**, and **10** to gain insight on the observed ligand folding. Each of the calculations revealed identical causality, and as such only calculation results for compound **5** are discussed here.

Ligand folding caused by steric effects from crystal packing was ruled out as geometry optimized calculations of complex **5** in the gas phase resulted in virtually no change in ligand fold angles. Using the crystal structure geometry as a template, the fold angle was changed to zero degrees and a single point DFT calculation was performed on this unfolded geometry so that direct comparisons of the electronic structures could be made between the folded and unfolded forms. Calculations reveal a total stabilization of 52 kcal/mol upon ligand folding in compound **5**, indicating that ligand folding is thermodynamically favorable. To determine the electronic nature of the stabilization, the NBOs (natural bond orbitals) were analyzed to determine individual orbital contributions. Several distinct contributions to the stabilizations were found to be important. First, an increase in sulfur/metal p-orbital overlap was seen with a subsequent 8 kcal/mol stabilization of the sulfur−metal σ bond. Metal dithiolenes are also known to behave in such a manner, often with large fold angles and significant metal−ligand covalency.[65] However, unlike metal-dithiolenes this orbital overlap is not the largest contributor to folding in the compounds studied here; rather, lone pair repulsion interactions are found to be most important. The largest repulsion is due to an interaction between the phosphorus and metal lone pair orbitals (Figure 2). This repulsion is lowered upon bending by a rotation of the phosphorus lone pair, resulting in a surprisingly large ∼30 kcal/mol stabilization. A smaller stabilization (∼5 kcal/mol) is also found by the reduction in overlap of the sulfur and metal lone pairs (Figure 2). In summary, NBO analysis of the DFT results leads to a description in the ligand fold being driven by (1) metal-S covalency, (2) metal-P lone pair repulsion, and (3) metal-S lone pair repulsion.

To gain more perspective on the significance of the sulfur/metal lone pair repulsion, the phenolate analogue **8** was prepared to determine how contracting the chalcogenide lone pair, and presumably decreasing lone pair repulsion, would affect the ligand folding. By replacing the S in **6** with O in **8**, a significant average fold angle decrease from 41.02 to 0.29 degrees was observed in the crystal structures (Figure 3). This dramatic decrease in fold angle is likely due to the oxygen/metal interaction leading to a relative decrease in metal/chalcogenide covalency.

With a more ionic chalcogenide/metal interaction one would expect a relative decrease in electron density and subsequent increase in Lewis acidity of the Sn center. This increase in acidity allows for a stronger Lewis acid−base interaction that is reflected in the shorter Sn−P bond lengths (2.84 and 2.87 Å) and the larger $^{1}J_{Sn-P}$ coupling constant (1256 Hz). Also, the stronger P lone pair donation shields the Sn center leading to a more upfield shift in the $^{119}Sn\{^{1}H\}$ NMR (−301.0 ppm).

The diphenyl analogue **7** also shows a significant structural difference from **5**, **6**, and **8** by exhibiting negative fold angles (average angle −44.11°). This geometry seen in the crystal structure can be attributed to $\pi-\pi$ interactions between phenyl rings on adjacent ligands (Supporting Information, Figure S2)

dx.doi.org/10.1021/ic400990n | Inorg. Chem. 2013, 52, 9875−9884

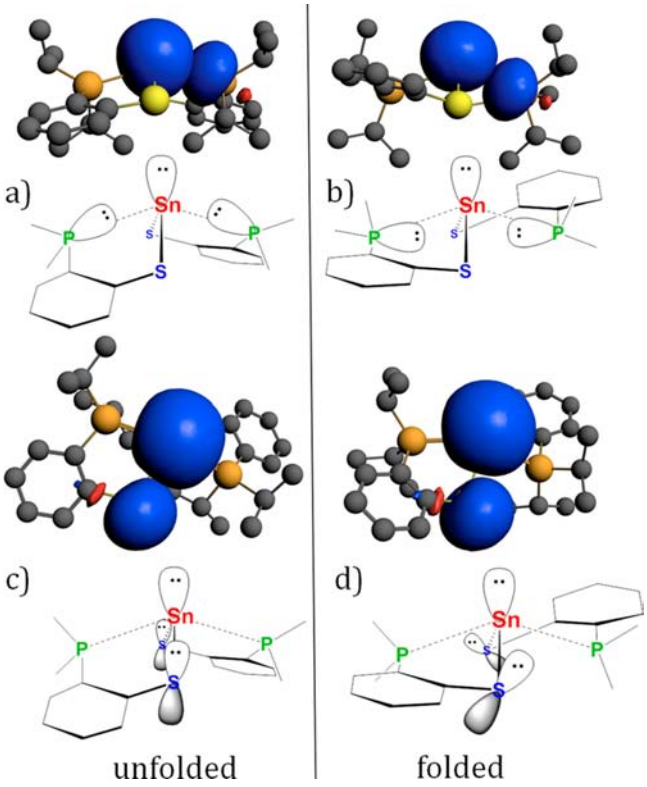

Figure 2. Calculated NBO orbitals for the Sn and P lone pairs on complex **5** in both the unfolded (a) and the folded geometries (b), and NBO orbitals for the Sn and S lone pairs on complex **5** in both the unfolded (c) and the folded geometries (d). Stick figure representations are shown to emphasize the rotation of both the P and S lone pairs upon ligand folding.

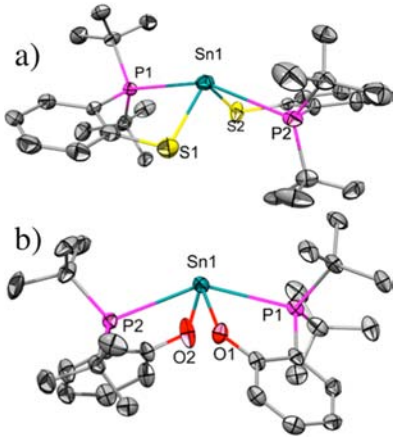

Figure 3. Molecular structures of **6** (a) and **8** (b) (50% ellipsoids). Hydrogen atoms omitted for clarity. Selected bond lengths (Å) and angles (deg). **6** (a): Sn(1)−P(1) 2.9217(19), Sn(1)−P(2) 3.0172(6), Sn(1)−S(1) 2.521(2), Sn(1)−S(2) 2.513(2), P(1)−Sn(1)−P(2) 152.002(10), S(1)−Sn(1)−S(1) 100.62(13). **8** (b): Sn(1)−P(1) 2.8444(16), Sn(1)−P(2) 2.8697(14), Sn(1)−O(1) 2.082(4), Sn(1)−O(2) 2.087(5), P(1)−Sn(1)−P(2) 145.00(5), O(1)−Sn(1)−O(2) 95.79(19).

with C−C distances between 3.5 and 3.6 Å, well within the normal range seen for such interactions.

Unlike the Sn(II) and Pb(II) complexes, the Zn(II) complexes **3** and **4** have no lone pair on the metal and as such adopt distorted tetrahedral coordination environments around the Zn atom (Figures 4 and Supporting Information, Figure S1) and also have relatively small fold angles (28.48 and

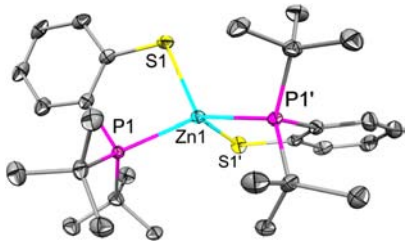

Figure 4. Molecular structure of **4** (50% ellipsoids). Hydrogen atoms omitted for clarity. Selected bond lengths (Å) and angles (deg). Zn(1)−P(1) 2.4225(9), Zn(1)−S(1) 2.3143(10), S(1)−Zn(1)−P(1) 90.14(3), S(1)−Zn(1)−S(1′) 117.87(6), P(1)−Zn-P(1′) 132.97(5), S(1)−Zn(1)−P(1′) 114.16(3).

18.78° for **3** and 14.39° for **4**). Again, all of the bond distances seen in **3** and **4**, including the directly bound atoms to Zn, fall in typically seen ranges and as such do not require any further comment.[23] The low fold angles observed in the crystal structures of **3** and **4** are consistent with our earlier findings suggesting that metal−sulfur and metal−phosphorus lone pair repulsions are the driving force behind large ligand fold angles. Only one fold angle is reported for **4** as it crystallized in the *C*2/*c* space group with a 2-fold rotation axis through the metal center.

Complexes **3**−**7** and **9**−**11** (as well as **12**−**15** described later) were reacted with gaseous CO_2 to attempt to form either CO_2 adducts or fully inserted products. The main group complexes were treated with bubbling CO_2 in CH_2Cl_2 solvent for 1 h at atmospheric pressure. Removal of the solvent followed by infrared spectroscopic characterization of the remaining solid product indicated no evidence of CO_2 addition to or reaction with the starting complexes. Characteristic C−O or C═O stretches were not present in the final products. This lack of reactivity was quite unexpected to us based on our previous work with other main group complexes,[17] but it may indicate the (undesired, in our case) strengths of the metal-heteroatom bonds in these various main group heterocyclic complexes.

Preparation and Characterization of Neutral Sn(IV) Complexes. The surprising lack of CO_2 reactivity in the Zn(II), Sn(II), and Pb(II) complexes **3**−**7** and **9**−**11** just mentioned encouraged us to seek alternate complexes using the same ligands, but with more acidic main group metal centers. Moving in this direction was prompted by the aforementioned work of Chapman et al. in which a cationic Zr(IV) complex employing an analogous phenolate ligand exhibited CO_2 reactivity.[18] As well, targeting a cationic Sn(IV) complex was viewed as ideal as it allows for direct comparisons with the Sn(II) complexes **5**−**7**. To obtain our targeted cationic Sn(IV) complex, we first needed to synthesize neutral Sn(IV) precursor complexes with labile chlorine substituents. These precursors revealed some interesting features meriting discussion separate from the targeted cationic Sn(IV) complexes.

For the syntheses of monoligated complexes **12** and **13**, a solution of either **1** or **2** in methanol was added dropwise to a stirred solution of Ph_2SnCl_2 and excess NEt_3, also in methanol, at −78 °C. An immediate reaction took place, resulting in the precipitation of the product as a white solid. As compared to reactions using Sn(II) described above, both lower temper-

dx.doi.org/10.1021/ic400990n | *Inorg. Chem.* 2013, 52, 9875−9884

atures and slow addition of the phosphinobenzenethiol were required to avoid adding two ligands to the tin center. Interestingly, when targeting the diphenyl analogue of **12** and **13** using 2-$Ph_2P(C_6H_4)SH$ under the same conditions, only the previously reported[27] doubly ligated compound $Sn\{(SC_6H_4\text{-}2\text{-}PPh_2)\text{-}\kappa\text{-}S\}_2Ph_2$ was formed.

The crystal structures of **12** and **13** revealed in both cases a distorted trigonal bipyramidal geometry around the tin atom. In both cases, the Cl occupies an axial position while both phenyl groups are in equatorial positions. Interestingly, a major difference occurs in the chelating ligand, as the P in **12** is in the equatorial position while in **13** it is found in the axial position (Figure 5).

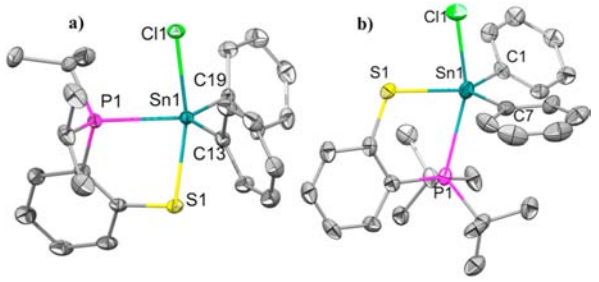

Figure 5. Molecular structures of **12** (a), and **13** (b) (50% ellipsoids). Hydrogen atoms omitted for clarity. Selected bond lengths (Å) and angles (deg). **11** (a): Sn(1)−P(1) 2.5564(3), Sn(1)−S(1) 2.5813(3), Sn(1)−Cl(1) 2.5438(3), Cl(1)−Sn(1)−S(1) 166.260(11), P(1)−Sn(1)−S(1) 79.906(10), C(19)−Sn(1)−C(13) 119.61(4), C(19)−Sn(1)−P(1) 119.54(3), C(13)−Sn(1)−P(1) 120.81(3). **12** (b): Sn(1)−P(1) 2.869(2), Sn(1)−S(1) 2.4292(17), Sn(1)−Cl(1) 2.5148(18), Cl(1)−Sn(1)−P(1) 159.44(6), S(1)−Sn(1)−P(1) 79.03(5), C(7)−Sn(1)−C(1) 115.3(2), C(7)−Sn(1)−S(1) 115.50(17), C(1)−Sn(1)−S(1) 129.12(19).

This difference in position of the P atom significantly changes the donor−acceptor characteristics of the Sn−P bond as evident from the Sn−P bond lengths and from the NMR spectra. In compound **12**, the P atom is in the equatorial plane with a Sn−P bond length of 2.5564(3) Å and a $^1J_{Sn-P}$ coupling constant of 637 Hz, showing sharp singlets in both the ^{119}Sn and ^{31}P NMR spectra. This is in clear contrast to **13**, which crystallizes with the P in the axial position and has a significantly longer Sn−P bond length of 2.869(2) Å. The ^{31}P NMR spectrum of analytically pure **13** shows two resonances: one very broad signal at 20.5 ppm and a sharp signal singlet at 71.2 ppm (Supporting Information, Figure S4). To confirm that the signals were coming from the same compound, a solid state ^{31}P NMR experiment was performed and revealed only one resonance at 12.9 ppm, indicating that in solution the Sn−P interaction is in fact dynamic.

The two signals showed differences in both resolution and in the Sn−P coupling constants. The broad signal at 20.5 ppm has a coupling constant of 389 Hz, while the sharp signal at 71.2 ppm has a coupling constant of 67 Hz. This is indicative of hemilability in the phosphine, where the signal at 20.5 ppm is consistent with the P in a weakly bound state and the signal at 71.2 ppm being unbound. The broadness of the signal and the larger coupling constant in the signal at 20.5 ppm supports this notion. A weakly bound P is more likely to become unbound in solution, and the coupling constant between P and Sn should reflect this as smaller in magnitude than a strongly bound P. The Sn−P coupling constant of **12** (637 Hz) serves as a good comparison as its Sn−P interaction is relatively stronger than that of **13**, as indicated by its shorter Sn−P bond length, its sharp signal in the ^{31}P NMR spectrum, and the absence of a second resonance in its ^{119}Sn and ^{31}P NMR spectra. The sharp signal at 71.2 ppm has a small coupling constant of 67 Hz, which if unbound would be a $^4J_{Sn-P}$ coupling. A paper by Weichmann et al.[66] reported $^4J_{Sn-P}$ coupling constants of 35 and 53 Hz in two similar Sn(IV) complexes. These complexes have phosphine ligands that are unbound in solution, but chelating in the solid state, as in complex **13** described above. The similarity in these values is additional evidence that the signal at 71.2 ppm is caused by an unbound P atom. Finally, to further substantiate the hemilability of the P,S chelate in **13**, a solution ^{31}P NMR spectrum was taken in the presence of a competing Lewis base. When pyridine was introduced into a solution of **13** in CH_2Cl_2, there was a drastic change in the relative signal intensity ratios (Supporting Information, Figure S4). The signal at 71.2 ppm became far more intense relative to the signal at 20.5 ppm after introduction of pyridine, indicative of an increase in concentration of unbound P. When pyridine was introduced in solution with **12**, no change in the ^{31}P NMR could be detected, indicating that pyridine could not compete with the strongly bound chelating phosphine for coordination to the tin.

Preparation and Characterization of Cationic Sn(IV) Complexes. Since complexes **12** and **13** had labile chlorine groups and an ancillary phosphinobenzenethiol ligand, the opportunity for the formation of stable Sn(IV) cations by halide abstraction seemed reasonable. Cations of heavier group 14 elements have garnered a lot of attention in recent years,[67−69] and the ability to isolate and characterize these cations has been aided by the development of robust, weakly coordinating anions, and/or ligands with high steric bulk.[68,70] Sn(IV) compounds, being Lewis acids and with the potential for hypercoordination, are particularly electrophilic.[71−73] This feature makes isolating cationic, coordinatively- and electronically unsaturated Sn(IV) species somewhat difficult. As such, there are only limited examples of isolated tricoordinate cationic Sn(IV) species,[68,69,74] each implementing steric bulk around the metal center to achieve ion stabilization. Examples of cationic Sn(IV) species with higher coordination numbers (>4) are much more common and often occur with stabilizing, tridentate ligands.[71,75,76] Tetracoordinate Sn(IV) cationic complexes, however, are scarce with only a few structurally characterized compounds available.[77−79] Of these compounds, only one prior example is monomeric, and with only one metal center ($[L^{CN}(^nBu)_2Sn]^+[Ti_2Cl_9]^-$, L^{CN} = 2-(*N*,*N*-dimethylaminomethyl)phenyl).[77] We have synthesized and structurally characterized a second example of this structural type by reacting **13** with $NaBPh_4$ in CH_2Cl_2 at room temperature for 15 h (Scheme 2 and Figure 6).

Scheme 2. Reaction Pathway for the Formation of 14 and 15

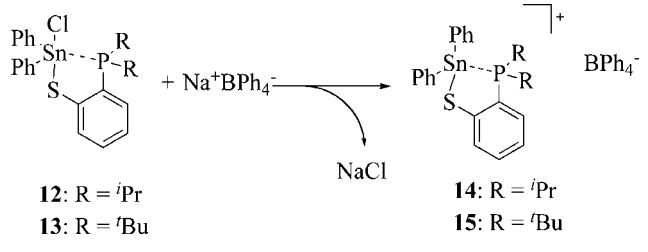

12: R = ^{i}Pr
13: R = ^{t}Bu
14: R = ^{i}Pr
15: R = ^{t}Bu

dx.doi.org/10.1021/ic400990n | *Inorg. Chem.* 2013, 52, 9875−9884

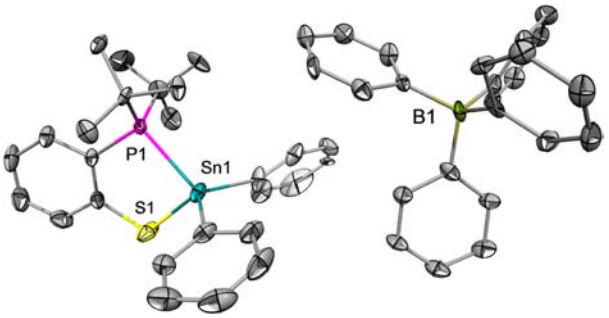

Figure 6. Molecular structure of **15** (50% ellipsoids). Hydrogen atoms omitted for clarity. Selected bond lengths (Å) and angles (deg). Sn(1)−P(1) 2.522(2), Sn(1)−S(1) 2.401(2), P(1)−Sn(1)−S(1) 87.89(8).

Attempts to grow single crystals suitable for the structure determination of **14** were not successful; however, NMR data and elemental analysis are consistent with the targeted product shown in Scheme 2. The choice of BPh_4^- as an anion in these syntheses stemmed from its lack of reactivity and weak coordinating ability, attributes which have made it an effective counterion in important catalysts in the past.[70,80] The crystal structure of **15**, revealed a 4-coordinate Sn complex with no signs of interaction between the metal center and the BPh_4^- counteranion or solvent (Figure 6).

The closest distance between the Sn and any part of the BPh_4^- anion is 5.170 Å, well outside the sum of the van der Waals radii for Sn and H. This complete isolation of the Sn(IV) cation is uncommon, as even anions with weak coordinating abilities such as $CF_3SO_3^-$, $AlCl_4^-$, and $Ti_2Cl_9^-$ have shown the propensity to interact with 4-coordinate cationic Sn(IV).[77,79,81] These interactions are apparent in the coordination geometry as the tetrahedral environment is perturbed when a weak interaction between the Sn and the anion moves the geometry toward trigonal bipyramidal, a perturbation not seen in **15**.

SUMMARY

Altering the sterics and electronics of donor atoms in unsymmetric multidentate ligands and characterizing their interaction with various metal centers is an important endeavor for the rational design of coordination compounds. We have thoroughly characterized many new varieties of main-group phosphinobenzenethiolates, discovering and rationalizing their traits. Main-group phosphinobenzenethiolates are far less explored than their transition-metal counterparts and are limited to the diphenylphosphino varieties. In fact there has only been one prior report of a metal dialkylphosphinobenzenethiolate where M = Ir or Rh and R = ^{i}Pr[31]. We have now extended the chemistry of the di-*i*-propyl derivative to several main-group metals and have also introduced the previously unreported di-*t*-butyl analogue. Also reported here, for the first time, is the description of ligand folding driven by metal/P and metal/S lone pair repulsions as well as by M-S covalency. In addition, this report includes an example of hemilability in which a room-temperature, dynamic interaction occurs between a Sn(IV) metal center and the P donor atom of the phosphinobenzenethiolate ligand. Lastly, a rare example of a stable, coordinatively unsaturated, cationic Sn(IV) complex is presented.

ASSOCIATED CONTENT

Supporting Information

Thermal ellipsoid plots of compounds **3**, **7**, and **10**, and ^{31}P NMR spectra for compound **13**. Crystallographic data in CIF format for compounds **3**−**10**, **12**, **13**, and **15** (CCDC 929503−929513). This material is available free of charge via the Internet at http://pubs.acs.org.

AUTHOR INFORMATION

Corresponding Author

*E-mail: rakemp@unm.edu.

Notes

The authors declare no competing financial interest.

ACKNOWLEDGMENTS

This work was financially supported by the National Science Foundation (Grants CHE09-11110 and CHE12-13529) and in part by the Laboratory Directed Research and Development (LDRD) program at Sandia National Laboratories (LDRD 151300). The Bruker X-ray diffractometer was purchased via a National Science Foundation CRIF:MU award to the University of New Mexico (CHE04-43580), and the NMR spectrometers were upgraded via grants from the NSF (CHE08-40523 and CHE09-46690). Sandia National Laboratories is a multiprogram laboratory managed and operated by Sandia Corporation, a wholly owned subsidiary of Lockheed Martin Corporation, for the United States Department of Energy's National Nuclear Security Administration under Contract DE-AC04-94AL85000.

REFERENCES

(1) Dilworth, J. R.; Wheatley, N. *Coord. Chem. Rev.* **2000**, *199*, 89.
(2) Bader, A.; Lindner, E. *Coord. Chem. Rev.* **1991**, *108*, 27.
(3) Slone, C. S.; Weinberger, D. A.; Mirkin, C. A. *Prog. Inorg. Chem.* **1999**, *48*, 233.
(4) Lee, W.-C.; Sears, J. M.; Enow, R. A.; Eads, K.; Krogstad, D. A.; Frost, B. J. *Inorg. Chem.* **2013**, *52*, 1737.
(5) Braunstein, P.; Naud, F. *Angew. Chem., Int. Ed.* **2001**, *40*, 680.
(6) Bassetti, M. *Eur. J. Inorg. Chem.* **2006**, *2006*, 4473.
(7) Garber, S. B.; Kingsbury, J. S.; Gray, B. L.; Hoveyda, A. H. *J. Am. Chem. Soc.* **2000**, *122*, 8168.
(8) Kingsbury, J. S.; Harrity, J. P. A.; Bonitatebus, P. J.; Hoveyda, A. H. *J. Am. Chem. Soc.* **1999**, *121*, 791.
(9) Angell, S. E.; Rogers, C. W.; Zhang, Y.; Wolf, M. O.; Jones, W. E. *Coord. Chem. Rev.* **2006**, *250*, 1829.
(10) Chung, K. H.; So, C. M.; Wong, S. M.; Luk, C. H.; Zhou, Z.; Lau, C. P.; Kwong, F. Y. *Chem. Commun.* **2012**, *48*, 1967.
(11) Lee, H. M.; Lee, C.-C.; Cheng, P.-Y. *Curr. Org. Chem.* **2007**, *11*, 1491.
(12) Objartel, I.; Ott, H.; Stalke, D. *Z. Anorg. Allg. Chem.* **2008**, *634*, 2373.
(13) Anderson, K. J.; Gilroy, J. B.; Patrick, B. O.; McDonald, R.; Ferguson, M. J.; Hicks, R. G. *Inorg. Chim. Acta* **2011**, *374*, 480.
(14) Dureen, M. A.; Stephan, D. W. *Dalton Trans.* **2008**, 4723.
(15) Robson, D. A.; Rees, L. H.; Mountford, P.; Schröder, M. *Chem. Commun.* **2000**, 1269.
(16) Dickie, D. A.; Coker, E. N.; Kemp, R. A. *Inorg. Chem.* **2011**, *50*, 11288.
(17) Chapman, A. M.; Haddow, M. F.; Wass, D. F. *Eur. J. Inorg. Chem.* **2012**, *2012*, 1546.
(18) Kraikivskii, P. B.; Frey, M.; Bennour, H. A.; Gembus, A.; Hauptmann, R.; Svoboda, I.; Fuess, H.; Saraev, V. V.; Klein, H.-F. *J. Organomet. Chem.* **2009**, *694*, 1869.
(19) Pérez-Lourido, P.; Romero, J.; García-Vázquez, J. A.; Sousa, A.; Zubieta, J.; Maresca, K. *Polyhedron* **1998**, *17*, 4457.

(20) Aznar, J.; Cerrada, E.; Hursthouse, M. B.; Laguna, M.; Pozo, C.; Romero, M. P. *J. Organomet. Chem.* **2001**, *622*, 274.
(21) Dilworth, J. R.; Morales, D.; Zheng, Y. *J. Chem. Soc., Dalton Trans.* **2000**, 3007.
(22) Fernandez, P.; Sousa-Pedrares, A.; Romero, J.; Duran, M. L.; Sousa, A.; Perez-Lourido, P.; Garcia-Vazquez, J. A. *Eur. J. Inorg. Chem.* **2010**, 814.
(23) Perez-Lourido, P.; Romero, J.; Garcia-Vazquez, J. A.; Sousa, A.; Maresca, K. P.; Zubieta, J. *Inorg. Chem.* **1999**, *38*, 3709.
(24) Perez-Lourido, P.; Romero, J.; Garcia-Vazquez, J. A.; Sousa, A.; Maresca, K.; Zubieta, J. *Inorg. Chem.* **1999**, *38*, 1293.
(25) Perez-Lourido, P.; Romero, J.; Garcia-Vazquez, J. A.; Sousa, A.; Zheng, Y.; Dilworth, J. R.; Zubieta, J. *J. Chem. Soc., Dalton Trans.* **2000**, 769.
(26) Perez-Lourido, P.; Romero, J.; Garcia-Vazquez, J. A.; Sousa, A.; Zubieta, J.; Russo, U. *J. Organomet. Chem.* **2000**, *595*, 59.
(27) Perez-Lourido, P.; Valencia, L.; Romero, J.; Garcia-Vazquez, J. A.; Sousa, A.; Zubieta, J. *Polyhedron* **2012**, *45*, 200.
(28) Vălean, A. M.; Gómez-Ruiz, S.; Lönnecke, P.; Silaghi-Dumitrescu, I.; Silaghi-Dumitrescu, L.; Hey-Hawkins, E. *Inorg. Chem.* **2008**, *47*, 11284.
(29) Aznar, J.; Cerrada, E.; Hursthouse, M. B.; Laguna, M.; Pozo, C.; Romero, M. P. *J. Organomet. Chem.* **2001**, *622*, 274.
(30) Canseco-González, D.; Gómez-Benítez, V.; Hernández-Ortega, S.; Toscano, R. A.; Morales-Morales, D. *J. Organomet. Chem.* **2003**, *679*, 101.
(31) Morales-Morales, D.; Rodriguez-Morales, S.; Dilworth, J. R.; Sousa-Pedrares, A.; Zheng, Y. *Inorg. Chim. Acta* **2002**, *332*, 101.
(32) Block, E.; Ofori-Okai, G.; Zubieta, J. *J. Am. Chem. Soc.* **1989**, *111*, 2327.
(33) Bornand, M.; Torker, S.; Chen, P. *Organometallics* **2007**, *26*, 3585.
(34) *APEX2*; Bruker AXS, Inc.: Madison, WI, 2007.
(35) Sheldrick, G. M. *Acta Crystallogr., Sect. A: Found. Crystallogr.* **2008**, *A64*, 112.
(36) Brandenburg, K. *Diamond*, 3.2i; Crystal Impact GbR: Bonn, Germany, 2012.
(37) te Velde, G.; Bickelhaupt, F. M.; van Gisbergen, S. J. A.; Fonseca Guerra, C.; Baerends, E. J.; Snijders, J. G.; Ziegler, T. *J. Comput. Chem.* **2001**, *22*, 931.
(38) Fonseca Guerra, C.; Snijders, J. G.; te Velde, G.; Baerends, E. J. *Theor. Chem. Acc.* **1998**, *99*, 391.
(39) *ADF2012.01*; SCM, Theoretical Chemistry, Vrije Universiteit: Amsterdam, The Netherlands; http://www.scm.com.
(40) van Lenthe, E.; Baerends, E. J. *J. Comput. Chem.* **2003**, *24*, 1142.
(41) van Lenthe, E.; Baerends, E. J.; Snijders, J. G. *J. Chem. Phys.* **1993**, *99*, 4597.
(42) van Lenthe, E.; Baerends, E. J.; Snijders, J. G. *J. Chem. Phys.* **1994**, *101*, 9783.
(43) van Lenthe, E.; Ehlers, A. E.; Baerends, E. J. *J. Chem. Phys.* **1999**, *110*, 8943.
(44) Glendening, E. D., Badenhoop, J. K., Reed, A. E., Carpenter, J. E., Bohmann, J. A., Morales, C. M., Weinhold, F. *NBO 5.0*; Theoretical Chemistry Institute, University of Wisconsin: Madison, WI, 2001.
(45) Foster, J. P.; Weinhold, F. *J. Am. Chem. Soc.* **1980**, *102*, 7211–7218.
(46) Figuly, G. D.; Loop, C. K.; Martin, J. C. *J. Am. Chem. Soc.* **1989**, *111*, 654.
(47) Hildebrand, A.; Lonnecke, P.; Silaghi-Dumitrescu, L.; Silaghi-Dumitrescu, I.; Hey-Hawkins, E. *Dalton Trans.* **2006**, 967.
(48) Cooney, J. J. A.; Cranswick, M. A.; Gruhn, N. E.; Joshi, H. K.; Enemark, J. H. *Inorg. Chem.* **2004**, *43*, 8110.
(49) Inscore, F. E.; Knottenbelt, S. Z.; Rubie, N. D.; Joshi, H. K.; Kirk, M. L.; Enemark, J. H. *Inorg. Chem.* **2006**, *45*, 967.
(50) Joshi, H. K.; Inscore, F. E.; Schirlin, J. T.; Dhawan, I. K.; Carducci, M. D.; Bill, T. G.; Enemark, J. H. *Inorg. Chim. Acta* **2002**, *337*, 275.
(51) Balz, H.; Kopf, H.; Pickardt, J. *J. Organomet. Chem.* **1991**, *417*, 397.
(52) Cranswick, M. A.; Dawson, A.; Cooney, J. J. A.; Gruhn, N. E.; Lichtenberger, D. L.; Enemark, J. H. *Inorg. Chem.* **2007**, *46*, 10639.
(53) Drew, S. C.; Hanson, G. R. *Inorg. Chem.* **2009**, *48*, 2224.
(54) Drew, S. C.; Young, C. G.; Hanson, G. R. *Inorg. Chem.* **2007**, *46*, 2388.
(55) Fourmigue, M. *Coord. Chem. Rev.* **1998**, *178–180* (Part 1), 823.
(56) Guyon, F.; Fourmigue, M.; Audebert, P.; Amaudrut, J. *Inorg. Chim. Acta* **1995**, *239*, 117.
(57) Guyon, F.; Fourmigue, M.; Clerac, R.; Amaudrut, J. *J. Chem. Soc., Dalton Trans.* **1996**, 4093.
(58) Joshi, H. K.; Enemark, J. H. *J. Am. Chem. Soc.* **2004**, *126*, 11784.
(59) Lauher, J. W.; Hoffmann, R. *J. Am. Chem. Soc.* **1976**, *98*, 1729.
(60) Reinheimer, E. W.; Olejniczak, I.; Lapinski, A.; Swietlik, R.; Jeannin, O.; Fourmigue, M. *Inorg. Chem.* **2010**, *49*, 9777.
(61) V. Jourdain, I.; Fourmigue, M.; Guyon, F.; Amaudrut, J. *J. Chem. Soc., Dalton Trans.* **1998**, 483.
(62) Whalley, A. L.; Blake, A. J.; Collison, D.; Davies, E. S.; Disley, H. J.; Helliwell, M.; Mabbs, F. E.; McMaster, J.; Wilson, C.; Garner, C. D. *Dalton Trans.* **2011**, *40*, 10457.
(63) Meskaldji, S.; Belkhiri, L.; Arliguie, T.; Fourmigue, M.; Ephritikhine, M.; Boucekkine, A. *Inorg. Chem.* **2010**, *49*, 3192.
(64) Roger, M.; Belkhiri, L.; Thuery, P.; Arliguie, T.; Fourmigue, M.; Boucekkine, A.; Ephritikhine, M. *Organometallics* **2005**, *24*, 4940.
(65) Kirk, M. L.; McNaugton, R. L.; Helton, M. E. *Prog. Inorg. Chem.* **2004**, *52*, 111.
(66) Weichmann, H. *J. Organomet. Chem.* **1984**, *262*, 279.
(67) Lee, V. Y.; Sekiguchi, A. *Acc. Chem. Res.* **2007**, *40*, 410.
(68) Schäfer, A.; Winter, F.; Saak, W.; Haase, D.; Pöttgen, R.; Müller, T. *Chem.—Eur. J.* **2011**, *17*, 10979.
(69) Sekiguchi, A.; Fukawa, T.; Lee, V. Y.; Nakamoto, M. *J. Am. Chem. Soc.* **2003**, *125*, 9250.
(70) Strauss, S. H. *Chem. Rev.* **1993**, *93*, 927.
(71) Jambor, R.; Dostál, L.; Růžička, A.; Císařová, I.; Brus, J.; Holčapek, M.; Holeček, J. *Organometallics* **2002**, *21*, 3996.
(72) Davis, M. F.; Clarke, M.; Levason, W.; Reid, G.; Webster, M. *Eur. J. Inorg. Chem.* **2006**, 2773.
(73) Kašná, B.; Jambor, R.; Dostál, L.; Kolářová, L.; Císarová, I.; Holeček, J. *Organometallics* **2005**, *25*, 148.
(74) Lambert, J. B.; Lin, L.; Keinan, S.; Müller, T. *J. Am. Chem. Soc.* **2003**, *125*, 6022.
(75) van Koten, G.; Jastrzebski, J. T. B. H.; Noltes, J. G.; Spek, A. L.; Schoone, J. C. *J. Organomet. Chem.* **1978**, *148*, 233.
(76) Thoonen, S. H. L.; van Hoek, H.; de Wolf, E.; Lutz, M.; Spek, A. L.; Deelman, B.-J.; van Koten, G. *J. Organomet. Chem.* **2006**, *691*, 1544.
(77) Turek, J.; Padelkova, Z.; Cernosek, Z.; Erben, M.; Lycka, A.; Nechaev, M. S.; Cisarova, I.; Ruzicka, A. *J. Organomet. Chem.* **2009**, *694*, 3000.
(78) Courtenay, S.; Ong, C. M.; Stephan, D. W. *Organometallics* **2003**, *22*, 818.
(79) Beckmann, J.; Dakternieks, D.; Duthie, A.; Mitchell, C. *Organometallics* **2003**, *22*, 2161.
(80) Hlatky, G. G.; Turner, H. W.; Eckman, R. R. *J. Am. Chem. Soc.* **1989**, *111*, 2728.
(81) MacDonald, E.; Doyle, L.; Burford, N.; Werner-Zwanziger, U.; Decken, A. *Angew. Chem., Int. Ed.* **2011**, *50*, 11474.